

Long non-coding RNA PTCSC3 suppresses triple-negative breast cancer by downregulating long non-coding RNA MIR100HG

GUOJUN ZHANG, LEI GAO, JUNLIANG ZHANG, RUI WANG and XIANGDONG WEI

Department of General Surgery, Changle People's Hospital, Changle County, Shandong 262499, P.R. China

Received December 19, 2018; Accepted September 13, 2021

DOI: 10.3892/ol.2023.13917

Abstract. Long non-coding RNA (lncRNA) PTCSC3 is characterized as a tumor suppressor in thyroid cancer and glioma. The present study aimed to investigate the role of PTCSC3 in triple-negative breast cancer (TNBC). A total of 82 patients with TNBC were enrolled in the present study. The results showed that PTCSC3 was downregulated, while lncRNA MIR100HG was upregulated in tumor tissues compared with that in adjacent non-cancerous tissues of patients with TNBC. The follow-up study showed that low expression levels of PTCSC3 and high expression levels of MIR100HG were closely associated with poor survival of patients with TNBC. The expression levels of MIR100HG were decreased with the clinic stages of TNBC, while the expression levels of PTCSC3 showed the opposite trend. Correlation analysis showed that the expression levels of PTCSC3 and MIR100HG were significantly correlated in both tumor tissues and adjacent non-cancerous tissues. The overexpression of PTCSC3 inhibited the expression level of MIR100HG in TNBC cells, while the expression level of PTCSC3 was unaffected. Cell Counting Kit-8 and Annexin V-FITC Apoptosis flow cytometry assays showed that overexpression of PTCSC3 led to inhibition, while overexpression of MIR100HG led to the promotion of TNBC cells viability and inhibited apoptosis of TNBC cells. In addition, overexpression of MIR100HG attenuated the effects of PTCSC3 overexpression on cancer cell viability. However, the overexpression of PTCSC3 did not affect cancer cell migration and invasion. Western-blot analysis showed that PTCSC3 suppressed viability and promoted apoptosis of TNBC cells through the Hippo signaling pathway. Thus, the present study demonstrated that lncRNA PTCSC3 inhibits cancer cell viability and promotes cancer cell apoptosis in TNBC by downregulating MIR100HG.

Introduction

The latest genome-wide transcriptome analyses revealed that ~2/3 of the genomic DNA of mammalian species is transcribed but >98% of the transcripts lack protein-coding capacity (1), indicating that most mammalian genes are non-protein coding genes. Long non-coding RNAs (lncRNAs) are a class of transcripts with pivotal biological functions in many processes (2), such as cell growth, embryonic development, and disease progression by regulating downstream genes at post-transcriptional and translational levels (3,4). Extensive studies have shown that lncRNAs play critical roles in cancer biology (5), and regulation of lncRNAs has shown potentials in inhibiting cancer development (6). However, functions of most lncRNAs are still unknown.

Although the mortality rate of breast cancer has dropped significantly during the past decades, it still accounts for >1/5 deaths among females (7). As a major subtype of breast cancer, triple-negative breast cancer (TNBC) is characterized by inhibited expression of estrogen receptor α , progesterone receptor, and human epidermal growth factor receptor 2 (8). The development and progression of TNBC involve the regulation of multiple lncRNAs (9,10). lncRNA PTCSC3 is characterized as a tumor suppressor in glioma and thyroid cancer, while its role in the recurrence of TNBC is unknown (11-13). It was reported that lncRNA MIR100HG promotes cell viability in TNBC (14). The interaction between different lncRNAs play important roles in tumor growth. For example, lncRNA PTCSC3 alleviates gastric cancer by regulating lncRNA HOXA11-AS (15). The present study investigated the involvement of PTCSC3 in TNBC and explored its potential interaction with MIR100HG. lncRNA PTCSC3 may serve as a target for the treatment and prognosis of gastric cancer.

Materials and methods

Research subjects. A total of 82 patients diagnosed with TNBC admitted at Changle People's Hospital between January 2010 and January 2013 were enrolled in the present study (Table I). The inclusion criteria included: i) Patients diagnosed by pathological biopsy; ii) patients diagnosed and treated for the first time; iii) patients who signed the informed consent. The exclusion criteria were as follows: i) Patients treated before admission; ii) patients diagnosed with multiple diseases, such as cardiovascular diseases, diabetes and gastroenteritis. The

Correspondence to: Dr Guojun Zhang, Department of General Surgery, Changle People's Hospital, 278 Limin Road, Changle County, Shandong 262499, P.R. China
E-mail: 2558486080@qq.com

Key words: triple-negative breast cancer, long non-coding RNA PTCSC3, long non-coding RNA MIR100HG, viability, apoptosis

age range of the 82 patients with TNBC was between 30 and 68 years old, and the mean age was 47.7 ± 5.0 years old. Based on AJCC staging, there were 25 cases at stage I, 24 cases at stage II, 19 cases at stage III and 14 cases at stage IV. The present study was approved by the Ethics Committee of Changde People's Hospital before the admission of patients. The ethics committee approval number is Changde-20160049.

Specimens and cell lines. Tumor tissues and adjacent non-cancerous tissues (3 cm away from the tumor tissue) were obtained from each patient through biopsy. All tissue specimens were confirmed by 3 experienced pathologists. Specimens were stored in liquid nitrogen before use.

BT-549 and HCC70 cell lines purchased from American Type Culture Collection were used for all *in vitro* cell experiments in the present study. Cells were cultivated in Roswell Park Memorial Institute (RPMI)-1640 medium (Gibco; Thermo Fisher Scientific, Inc.) containing 10% FBS (Gibco; Thermo Fisher Scientific, Inc.) and 0.023 IU/ml insulin at 37°C with 5% CO₂.

Follow-up. All patients were followed-up for 5 years from the day of admission to record their overall survival conditions.

Total RNA extraction and reverse transcription-quantitative polymerase chain reaction (RT-qPCR). Tissue specimens were ground in liquid nitrogen. RNAzol reagent (Sigma-Aldrich; Merck KGaA) was used to extract total RNAs from tissue specimens and *in vitro* cultivated cells. SuperScript IV Reverse Transcriptase (Thermo Fisher Scientific, Inc.) was used to synthesize cDNA through reverse transcription (gentle mixing and incubation at 37°C for 2 min, followed by incubation of the sample for 15 min at 55°C in the presence of 10 mM dithiothreitol to inactivate the enzyme). To detect the expression levels of PTCSC3 and MIR100HG, SYBR[®] Green Quantitative RT-qPCR (Sigma-Aldrich; Merck KGaA) was used to prepare all PCR reactions. The PCR reaction conditions were: 55 sec at 95°C, followed by 12 sec at 95°C and 32 sec at 58.5°C for 40 cycles. PCRs were performed on an ABI 7500 System. 18S RNA was used as the endogenous control. Primers of PTCSC3 and MIR100HG as well as 18S RNA were designed and synthesized by Sangon Biotech Co., Ltd. The expression levels of PTCSC3 and MIR100HG were normalized to 18S RNA using 2^{-ΔΔCq} method (16). The primer sequences were listed as follows: lncRNA PTCSC3 forward, 5'-CCAGGGGATCGCATTTTTC-3'; lncRNA PTCSC3 reverse, 5'-CTTCTGCTTGGCCTTTGACC-3'; lncRNA MIR100HG forward, 5'-TCGAACCTTGGAGTGTGGCA-3'; lncRNA MIR100HG reverse, 5'-TCCCTGGTTACTGCCAGAT-3'; 18S RNA forward, 5'-CGGCTACCACATCCAAGGAA-3'; 18S RNA reverse, 5'-TGCTACTACCTCCCCGTGTCA-3'.

Vectors and cell transfection. The vector expressing PTCSC3 or MIR100HG were designed using pcDNA3.1 vector as backbone that was synthesized by Sangon Biotech Co., Ltd. BT-549 and HCC70 cells were seeded in 6-well plates (1x10⁵ cells/well) and transfected with 10 nM vector using Lipofectamine[®] 2000 reagent (cat. no. 11668-019; Invitrogen; Thermo Fisher Scientific, Inc.). Cells transfected with the empty vectors were used as negative control cells. Non-transfected

Table I. Clinical characteristics of patients with triple-negative breast cancer.

Characteristics	Number	Percentage
Age, years		
≤50	45	54.9
≥50	37	45.1
Stage		
I	25	30.5
II	24	29.3
III	19	23.2
IV	14	17.0
Patients not treated	73	89.0
Patients treated for the first time (arubicin + paclitaxel)	9	11.0

cells treated with Lipofectamine[®] 2000 reagent only were used as the control cells. Cells were harvested at 24 h after transfection for subsequent experiments.

Western blotting. Total protein was isolated from cells using RIPA buffer reagent (Thermo Fisher Scientific, Inc.) containing protease inhibitor (Cocktail, Roche Diagnostics). The protein concentration was measured using a BCA assay kit (Thermo Fisher Scientific, Inc.). The same amount of protein samples (30 μg) were separated by 10% SDS-PAGE (Shanghai Enzyme Link Biotechnology Co., Ltd.) and transferred onto nitrocellulose membranes (GE Healthcare). Blocking was performed using 5% BSA at room temperature for 2 h. GAPDH was selected as the housekeeping protein for general western blotting. The protein-membrane was incubated with the primary antibodies of anti-phosphorylated (p)-LATS1 (1:1,000; cat. no. ab111344; Abcam), anti-LATS1 (1:1,000; cat. no. ab243656; Abcam), anti-p-YAP (1:1,000; cat. no. ab76252; Abcam), anti-Yes-associated protein (YAP; 1:1,000; cat. no. ab52771; Abcam) and anti-GAPDH (1:1,000; cat. no. ab8245; Abcam) at 4°C overnight. For the detection of nuclear YAP, laminB was selected as the internal control, and the membranes were also incubated with anti-nuclear YAP antibody (1:1,000; cat. no. ab52771; Abcam) and anti-laminB (1:1,000; cat. no. ab16048; Abcam) at 4°C overnight. TBST buffer was used to elute the membrane twice. The membranes were then incubated with the secondary antibody [Goat Anti-Rabbit IgG H&L (HRP) preadsorbed; cat. no. ab7090; dilution, 1:5,000; Abcam; or Goat Anti-Mouse IgG+IgM H&L (HRP) preadsorbed; cat. no. ab47827; dilution, 1:5,000; Abcam] at 37°C for 2 h. The ECL detection system (Thermo Fisher Scientific, Inc.) was used to detect the protein bands. ImageJ software v.1.51j8 (National Institutes of Health) was used for densitometry analyses.

In vitro cell viability assay. *In vitro* cell viability assay was carried out using Cell Counting Kit-8 kit (CCK-8; cat. no. ab228554, Abcam) to detect cell viability at 24 h post transfection. Briefly, single cell suspensions were prepared using RPMI-1640 medium and cell density was adjusted to

5×10^4 cells/ml. Cells were cultivated in a 96-well plate with $100 \mu\text{l}$ cell suspension per well at 37°C with $5\% \text{CO}_2$. CCK-8 solution ($10 \mu\text{l}$) was added at 24, 48, 72 and 96 h after the beginning of cell culture. Subsequently, cells were cultivated for an additional 4 h and $10 \mu\text{l}$ dimethyl sulfoxide (DMSO) was added. OD values at 450 nm were used to reflect cell viability abilities.

Cell invasion and migration assays. BT-549 and HCC70 cells were seeded onto the upper chamber of Transwell inserts ($8 \mu\text{m}$ pore; Corning, Inc.) with 3,000 cells in 0.1 ml non-serum medium per well. The lower chamber of the Transwell was filled with medium supplemented with 20% FBS. Matrigel-coated membrane was used in invasion assay. Cells were cultured at 37°C with $5\% \text{CO}_2$ for 12 h. Subsequently, the upper surface of membrane was cleaned, and 0.5% crystal violet (Sigma-Aldrich; Merck KGaA) was used to stain the cells in the lower surface at 25°C for 30 min. The stained cells were observed under an optical microscope (magnification, $\times 100$; Olympus DX51; Olympus Corporation). All cell groups were normalized to the control (C) group.

Cell apoptosis assay. Cell apoptosis was determined by flow cytometry using Annexin V-FITC Apoptosis Detection kit (BD Biosciences). Briefly, BT-549 and HCC70 cells were seeded in 6-well plates (1×10^5 cells/well) and incubated for 24 h at 37°C with $5\% \text{CO}_2$. Cells were collected and washed by PBS. Then, cells were re-suspended in $200 \mu\text{l}$ binding buffer containing $5 \mu\text{l}$ Annexin V-FITC and $10 \mu\text{l}$ propidium iodide (PI) and further incubated for 30 min at room temperature. Cell apoptosis was detected by a flow cytometer (BD Bioscience).

BrdU staining. BrdU staining was used to monitor cell viability. Briefly, BT-549 and HCC70 cells were inoculated into 24-well plates (10,000 cells/well) and cultured at 37°C overnight. Following 48 h, $10 \mu\text{g/ml}$ BrdU was added to the medium and incubated for 2 h at room temperature, followed by cell fixation using 4% paraformaldehyde for 15 min at room temperature. Following treatment with 2 M HCL and 0.3% Triton X100, cells were blocked with 10% goat serum (ZSGB-Bio). Cells were then incubated with BrdU primary antibody (cat. no. A1482; mouse anti-BrdU primary antibody; dilution, 1:50; lot. 347580; BD Biosciences) and then secondary antibody (FITC-conjugated rabbit anti-mouse secondary antibody; dilution, 1:25; cat. no. FI-2000; Vector Laboratories, Inc.). Cells were then stained with DAPI for 30 min at room temperature. BrdU-positive cells were counted in three random areas under a Leica confocal microscope (TCS SP8; Leica Microsystems, Inc.).

Immunofluorescence staining. BT-549 and HCC70 cells were fixed in 4% paraformaldehyde for 15 min at room temperature and then permeabilized in 0.1% Triton X-100 at room temperature for 20 min. Cardiomyocytes were then blocked in PBS containing 0.5% bovine serum albumin at 37°C for 60 min and incubated with primary rabbit antibody against YAP (cat. no. ab52771; 1:200, Abcam) at 4°C overnight, followed by incubation with Alexa Fluor 488-conjugated anti-rabbit IgG secondary antibody (dilution, 1:3,000; cat. no. A-11034; Invitrogen; Thermo Fisher Scientific, Inc.). Finally, the nuclei

were stained with DAPI for 30 min at room temperature. Images were visualized and captured with a Leica SP8 confocal microscopy (magnification, $\times 200$; Leica Microsystems, Inc.).

Nuclear/cytoplasmic fractionation. For nuclear YAP accumulation assay, BT-549 and HCC70 cells were harvested and lysed to obtain cytoplasmic and nuclear lysates using the Keygen Nuclear-Cytosol Protein Extraction kit (Nanjing KeyGen Biotech. Co., Ltd.). Western blotting was performed to detect the cytoplasmic and nuclear lysates.

Statistical analyses. All experiments were repeated for 3 times and data of 3 replicates were used to calculate the mean \pm standard deviation (SD). Statistical analyses were performed using GraphPad Prism 6 software (GraphPad Software Inc.). Comparison of the expression levels of PTCSC3 and MIR100HG between tumor and non-cancerous tissues was performed by paired Student's t-test. Comparison of the expression levels of PTCSC3 and MIR100HG in cells with different treatments, as well as cell viability, apoptosis and migration data, were performed by one-way ANOVA and Tukey's test. Correlations between the expression levels of PTCSC3 and MIR100HG were analyzed by Pearson's correlation coefficient. According to Youden's index, patients were divided into high ($n=38$) and low ($n=44$) PTCSC3 groups, as well as high ($n=36$) and low ($n=46$) MIR100HG level groups. Kaplan-Meier method was used to plot survival curves, which were compared by log-rank test. $P < 0.05$ as considered to indicate a statistically significant difference.

Results

Expression levels of PTCSC3 and MIR100HG are altered in TNBC tissues. The expression levels of PTCSC3 and MIR100HG in both tumor tissues and adjacent non-cancerous tissues of the 82 patients with TNBC were detected by RT-qPCR. Comparison of the expression levels of PTCSC3 and MIR100HG between tumor and non-cancerous tissues were performed by paired Student's t-test. PTCSC3 was significantly downregulated (Fig. 1A), while lncRNA MIR100HG was significantly upregulated (Fig. 1B) in tumor tissues compared with adjacent non-cancerous tissues of patients with TNBC ($P < 0.05$).

Expression levels of PTCSC3 and MIR100HG in tumor tissues predicts survival of patients with TNBC. According to Youden's index, patients were divided into high ($n=38$) and low ($n=44$) PTCSC3 groups, as well as high ($n=36$) and low ($n=46$) MIR100HG level groups. As shown in Fig. 2A, the survival rate of patients in the low level PTCSC3 group was significantly lower compared with that of patients in the high level PTCSC3 group ($P=0.0013$). In contrast, the survival rate of patients in the high level MIR100HG group was significantly lower compared with that of patients in the low level MIR100HG group (Fig. 2B; $P=0.0225$). Based on the role of PTCSC3 and MIR100HG in the survival of TNBC, Cox proportional hazard model was used to compare the importance of lncRNA PTCSC3 and MIR100HG with SNHG22 and H19 (17,18). PTCSC3 and MIR100HG had independent significance for the survival rate of patients with TNBC (Table II).

Table II. Cox analysis of prognosis of patients with triple-negative breast cancer.

Factors	β	SE	P-value	RR	95% CI
PTSCSC3	1.909	0.371	<0.001	0.148	0.072-0.307
MIR100HG	1.688	0.584	0.004	0.185	0.059-0.581
SNHG22	2.198	0.637	0.001	0.111	0.032-0.387
H19	1.004	0.344	<0.001	0.366	0.213-0.629

RR, relative risk; SE, standard error.

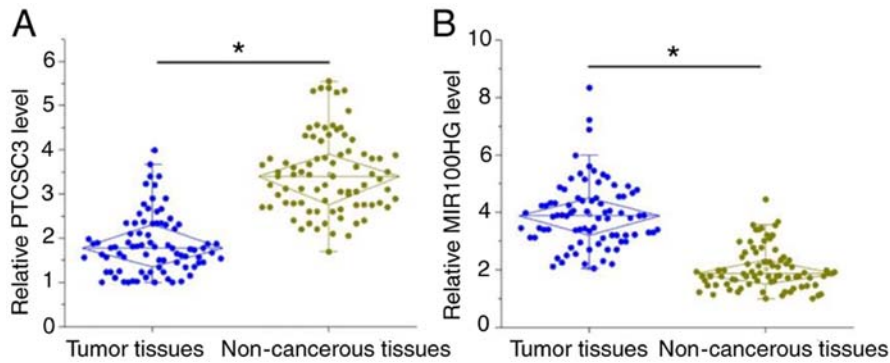


Figure 1. Expression level of PTSCSC3 and MIR100HG are altered in TNBC tissues. Reverse transcription-quantitative PCR results showed that PTSCSC3 was significantly downregulated, (A) while long non-coding RNA MIR100HG was significantly upregulated (B) in tumor tissues compared with that in adjacent tumor tissues of patients with TNBC. * $P < 0.05$. TNBC, triple-negative breast cancer.

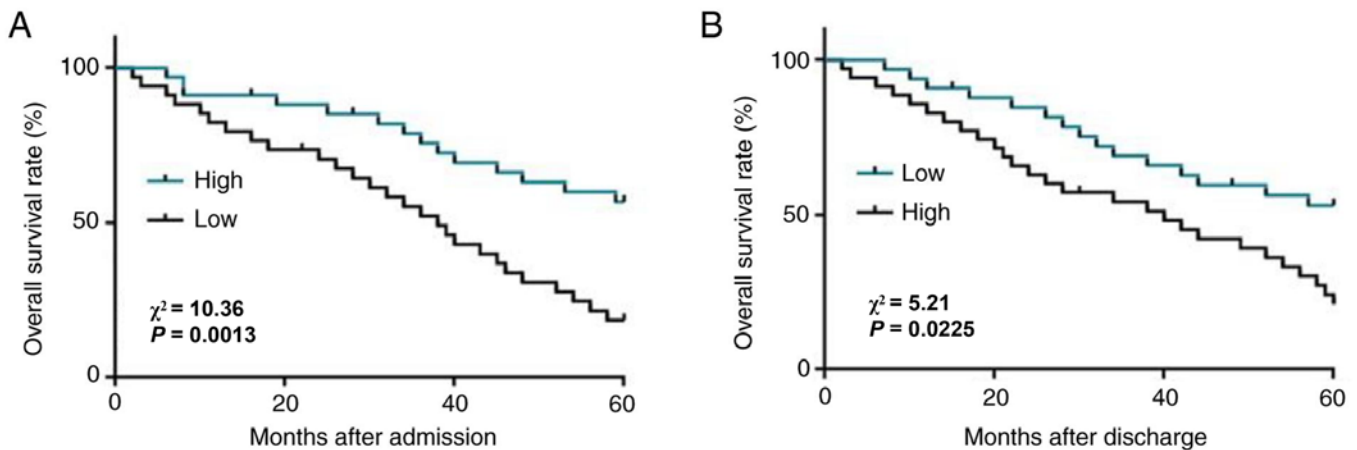


Figure 2. Expression level of PTSCSC3 and MIR100HG in tumor tissues predicts survival of patients with TNBC. Follow-up study and survival curve analysis showed that low level of PTSCSC3 (A) and high level of MIR100HG (B) were closely associated with poor survival of patients with TNBC. TNBC, triple-negative breast cancer.

Expression levels of PTSCSC3 and MIR100HG are inversely correlated. The expression levels of PTSCSC3 and MIR100HG in tumor tissues were detected according to the different stages of 82 patients with TNBC. The expression levels of PTSCSC3 was significantly decreased in stage II compared with that in stage I, and there was no significant difference in expression between stages II and III or between stages III and IV (Fig. 3A; $P < 0.05$). However, the expression levels of MIR100HG significantly increased in stage II, and remained unchanged at stages III and IV (Fig. 3B; $P < 0.05$). Correlations between

the expression levels of PTSCSC3 and MIR100HG were then analyzed by Pearson's correlation coefficient and a significantly inverse correlation was found between tumor tissues (Fig. 3C) and adjacent non-cancerous tissues (Fig. 3D).

PTSCSC3 is an upstream inhibitor of MIR100HG in TNBC cells. To further assess the interaction between PTSCSC3 and MIR100HG, PTSCSC3 and MIR100HG overexpression vectors were transfected into BT-549 and HCC70 cells; overexpression was confirmed at 24 h after transfection (Fig. 4A; $P < 0.05$).

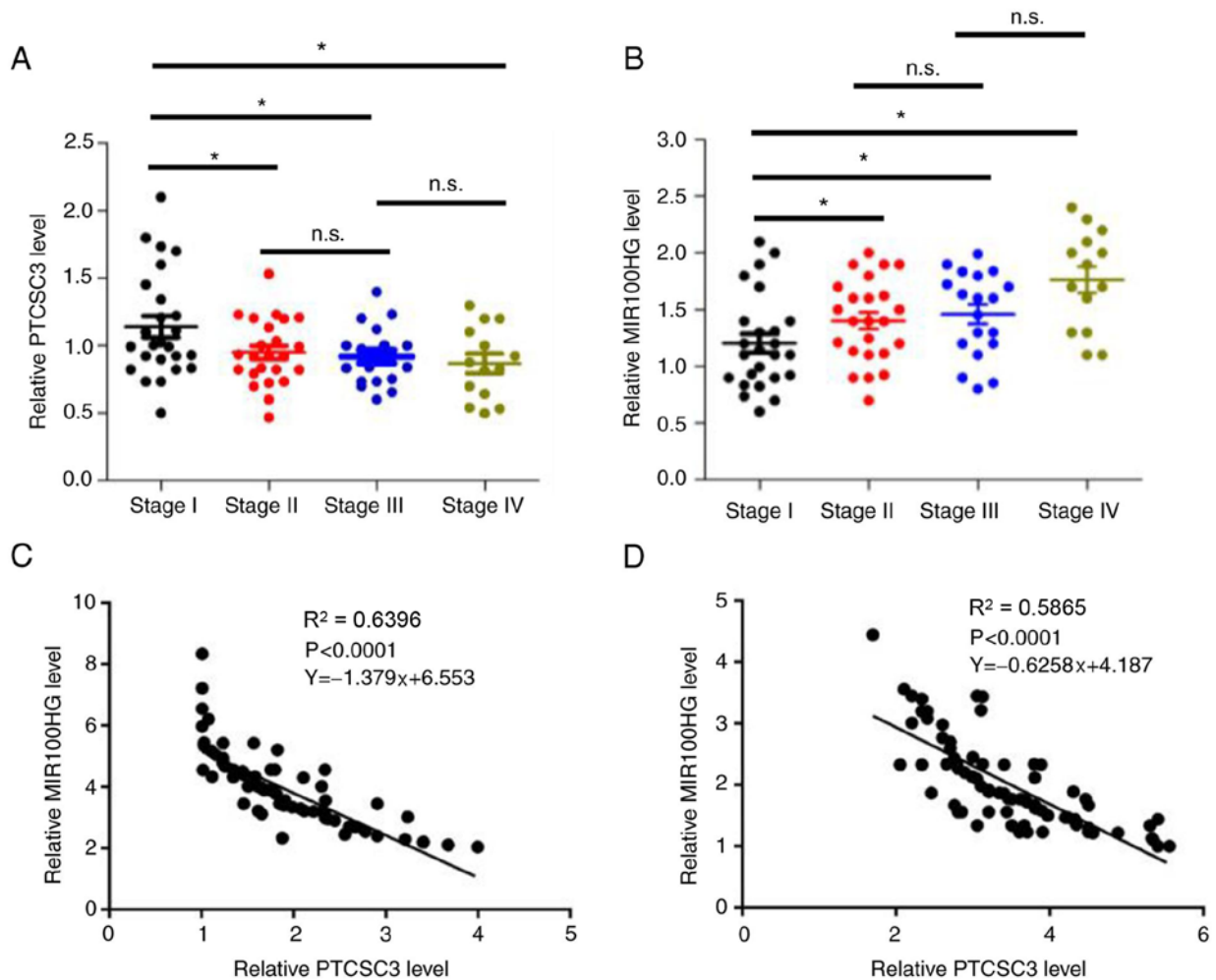


Figure 3. Expression levels of PTSCSC3 and MIR100HG are inversely correlated. Reverse transcription-quantitative PCR results showed that PTSCSC3 (A) and long non-coding RNA MIR100HG (B) expression levels varied at the different stages of triple-negative breast cancer. Correlation analysis showed that expression levels of PTSCSC3 and MIR100HG were significantly and negatively correlated in both tumor tissues (C) and adjacent tumor tissues (D). * $P < 0.05$.

Compared with the C and NC groups, overexpression of PTSCSC3 inhibited the expression level of MIR100HG in cells of both cell lines (Fig. 4B; $P < 0.05$). In contrast, overexpression of MIR100HG did not affect the expression level of PTSCSC3 (Fig. 4C).

Overexpression of PTSCSC3 inhibits viability and promotes apoptosis of TNBC cells through MIR100HG. Compared with the C and NC groups, overexpression of PTSCSC3 inhibited, while overexpression of MIR100HG promoted the viability of TNBC BT-549 (Fig. 5A) and HCC70 (Fig. 5B) cells ($P < 0.05$). In addition, rescue experiments showed that overexpression of MIR100HG attenuated the effects of overexpression of PTSCSC3 on cancer cell viability ($P < 0.05$). Cell apoptosis assay showed increased apoptosis rate in cancer cells with the overexpression of PTSCSC3 compared with that in the C group ($P < 0.01$), while overexpression of PTSCSC3 and MIR100HG reversed the effect of overexpression of PTSCSC3 in BT-549 (Fig. 5C) and HCC70 (Fig. 5D) ($P < 0.05$). In addition, BrdU staining assay results showed that PTSCSC3 increased cell viability and MIR100HG had the opposite effect. Also, overexpression of PTSCSC3 and MIR100HG reversed the effect of PTSCSC3 overexpression in BT-549 (Fig. 5E) and HCC70

(Fig. 5F) ($P < 0.05$). However, the overexpression of PTSCSC3 and MIR100HG did not affect cancer cell migration and invasion in BT-549 (Fig. 5G) and HCC70 (Fig. 5H) cells.

PTSCSC3 suppresses viability and promotes apoptosis of TNBC cells through the Hippo signaling pathway. Hippo signaling pathway plays a key role in cancer progression. Western blot analysis demonstrated that overexpression of PTSCSC3 was associated with increased p-YAP/YAP and p-LATS1/LATS1, while overexpression of MIR100HG was associated with decreased p-YAP/YAP and p-LATS1/LATS1 in TNBC BT-549 (Fig. 6A) and HCC70 (Fig. 6C) cells ($P < 0.05$). In addition, overexpression of MIR100HG attenuated the effect of PTSCSC3 on p-YAP/YAP and p-LATS1/LATS1 (Fig. 6A and C; $P < 0.05$). Nucleus/cytoplasm fractionation and western blot analysis revealed that the nuclear expression levels of YAP were decreased following overexpression of PTSCSC3, while these were increased following overexpression of MIR100HG in BT-549 (Fig. 6B) and HCC70 (Fig. 6D) cells ($P < 0.05$). In addition, the overexpression of MIR100HG attenuated the effect of PTSCSC3 on the nuclear expression levels of YAP (Fig. 6B and D; $P < 0.05$). The effects of PTSCSC3 and MIR100HG on the nuclear expression levels of YAP were

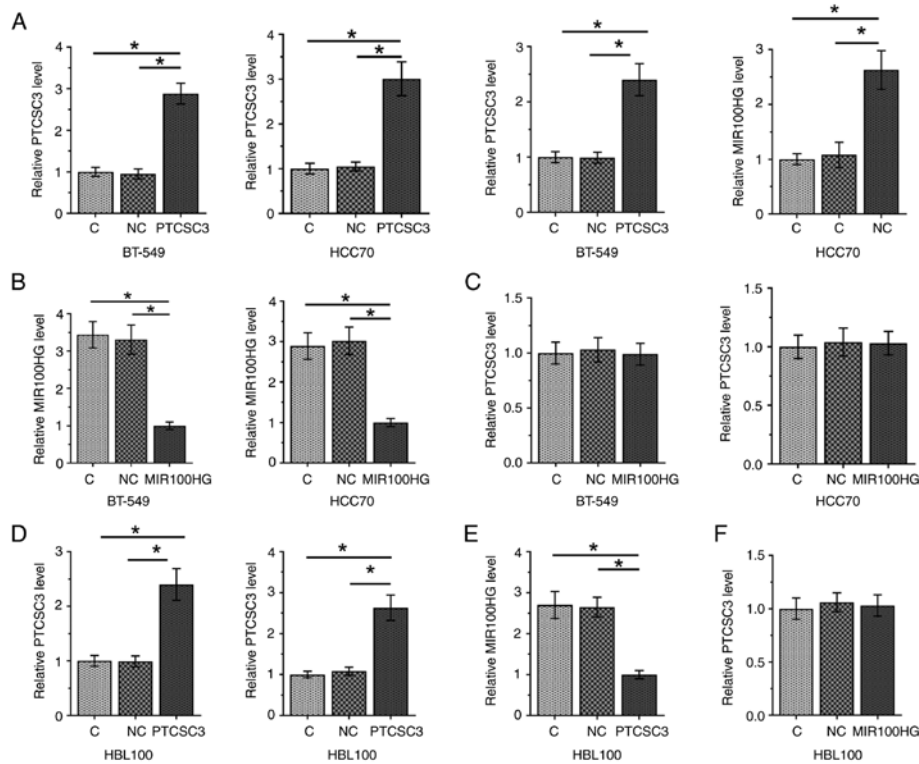


Figure 4. PTSCSC3 is an upstream inhibitor of MIR100HG in TNBC cells. Overexpression of PTSCSC3 and MIR100HG was achieved at 24 h after transfection. (A) Overexpression of PTSCSC3 inhibited the expression of MIR100HG in TNBC cells, (B) while overexpression of MIR100HG did not affect the expression of PTSCSC3 (C) ($P < 0.05$). Overexpression of PTSCSC3 and MIR100HG was achieved at 24 h after transfection. (D) Overexpression of PTSCSC3 inhibited the expression of MIR100HG in TNBC cells, (E) while overexpression of MIR100HG did not affect the expression of PTSCSC3 (F). * $P < 0.05$. TNBC, triple-negative breast cancer; C, control; NC, negative control.

confirmed by immunofluorescence assays in BT-549 (Fig. 6E) and HCC70 (Fig. 6F) cells.

Discussion

lncRNA PTSCSC3 is characterized as a tumor suppressor in thyroid cancer and glioma, while its involvement in other types of cancer is unknown. The key finding of the present study is that PTSCSC3 is downregulated in TNBC and may play a tumor suppressive role in TNBC by downregulating MIR100HG, which is an oncogenic lncRNA in TNBC. A recent study reported that MIR100HG is upregulated in TNBC and is correlated with increased viability of cancer cells (19). Consistent with previous study (20), the present study also observed upregulated expression of MIR100HG in TNBC tissues compared with that in adjacent non-cancerous tissues; and upregulation of MIR100HG significantly promoted TNBC cell viability. Besides, the follow-up study also showed that the high expression levels of MIR100HG in tumor tissues is significantly correlated with the poor survival of patients with TNBC. Therefore, MIR100HG may serve as a prognostic marker for TNBC.

lncRNAs exert their biological functions by regulating downstream oncogenic and tumor suppression pathways, such as the MTDH-Twist1 signaling, Akt signaling and other non-coding RNAs such as miRNAs (21,22). However, interactions between lncRNAs have not been well-studied. One study demonstrated the crosstalk of lncRNA PTSCSC3 and lncRNA H19 in TNBC, proved the interactions between different

lncRNAs, while the association of PTSCSC3 and MIR100HG and their downstream pathways are unknown (23). In the present study, it was demonstrated that PTSCSC3 is likely an upstream inhibitor of MIR100HG in TNBC cells, and downregulation of MIR100HG by PTSCSC3 is shown to participate in the regulation of cancer cell viability and apoptosis. MIR100HG was a well-characterized oncogenic lncRNA in different types of cancer. The inhibition of MIR100HG could serve as a therapeutic target for cancer treatment by inhibiting cancer cell viability, migration and invasion (24,25). In the development of TNBC, MIR100HG was upregulated and resulted in promoted progression of TNBC by sponging miR-5590-3p or regulating P27 (20). In the present study, significantly upregulated expression of MIR100HG in tumor tissues of patients with TNBC was observed. In addition, the *in vitro* cell viability and apoptosis assays also suggested the regulatory role of MIR100HG in TNBC cells. The present study further confirmed the oncogenic role of MIR100HG in TNBC.

lncRNA PTSCSC3 is known as a tumor suppressor in thyroid cancer and gastric cancer. For instance, in thyroid cancer, PTSCSC3 is downregulated in the plasma of patients with gastric cancer and can regulate multiple pathways, such as the Wnt and STAT3 signaling pathway, to impact cancer cellular behaviors including viability, migration and invasion (12,26,27). In addition, PTSCSC3 is downregulated in gastric cancer and can interact with lncRNA HULC, HOXA11-AS and Linc-pint to suppress invasion and viability of cancer cells (28,29). Moreover, recent studies suggested that PTSCSC3 is a potential biomarker for the

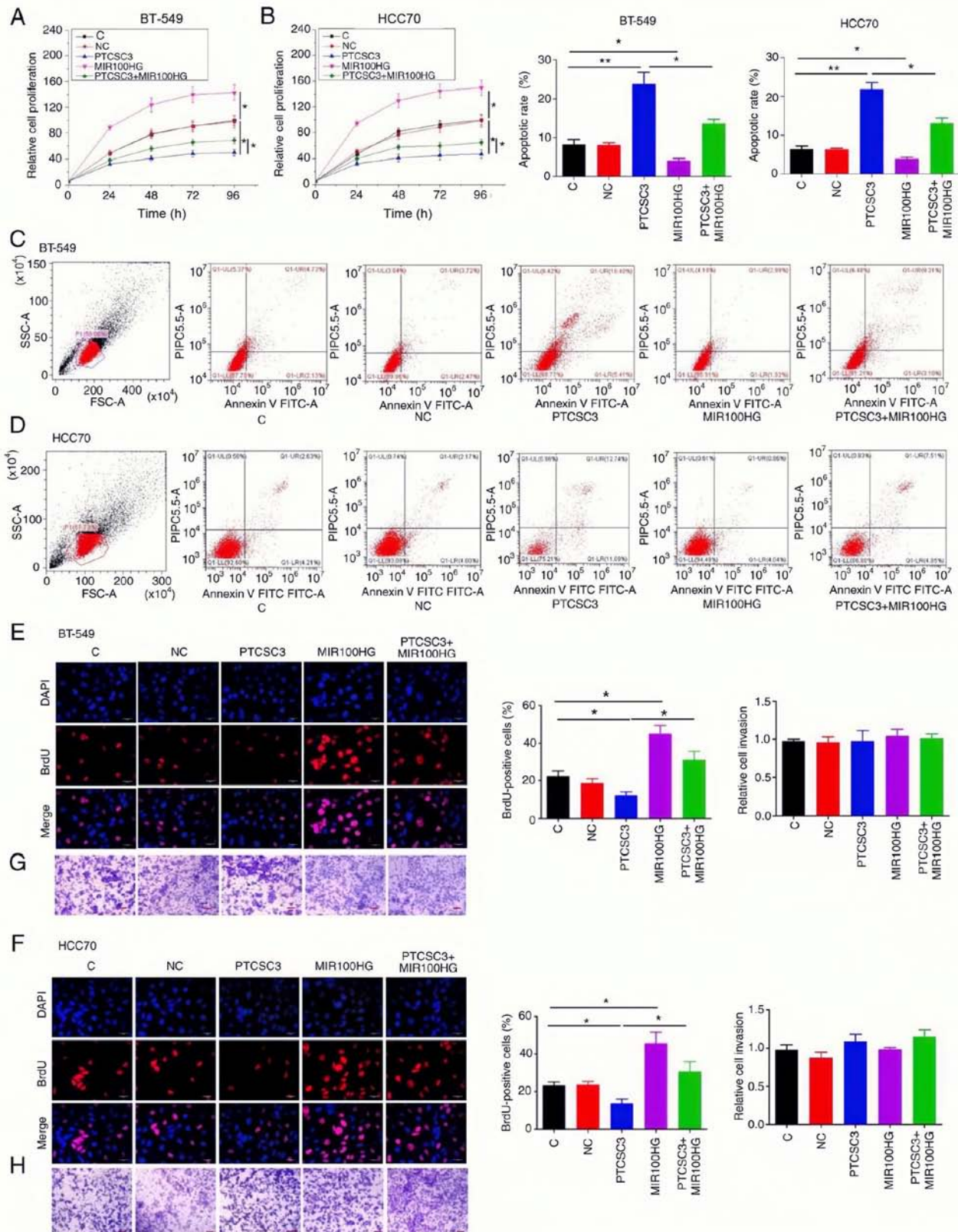


Figure 5. Overexpression of PT CSC3 inhibits viability and promotes apoptosis of TNBC cells through MIR100HG. Overexpression of PT CSC3 led to inhibited, while overexpression of MIR100HG led to promoted viability of TNBC BT-549 (A) and HCC70 (B) cells. In addition, rescue experiments showed that overexpression of MIR100HG attenuated the effects of PT CSC3 overexpression on cancer cell viability. Overexpression of PT CSC3 led to promoted, while overexpression of MIR100HG led to inhibited viability of TNBC BT-549 (C) and HCC70 (D) cells. Overexpression of MIR100HG attenuated the effects of PT CSC3 overexpression on cancer cell apoptosis. Moreover, BrdU was used for staining to further detect the TNBC cell viability. Overexpression of PT CSC3 inhibited, while overexpression of MIR100HG promoted the viability of TNBC BT-549 (E) and HCC70 (F) cells by BrdU staining. In addition, rescue experiments showed that overexpression of MIR100HG attenuated the effects of PT CSC3 overexpression on cancer cell viability. Scale bars, 30 μ m. Overexpression of PT CSC3 and MIR100HG did not affect the migration of TNBC BT-549 (G) and HCC70 (H) cells. Scale bars, 100 μ m. **P<0.01; *P<0.05. TNBC, triple-negative breast cancer; C, control; NC, negative control.

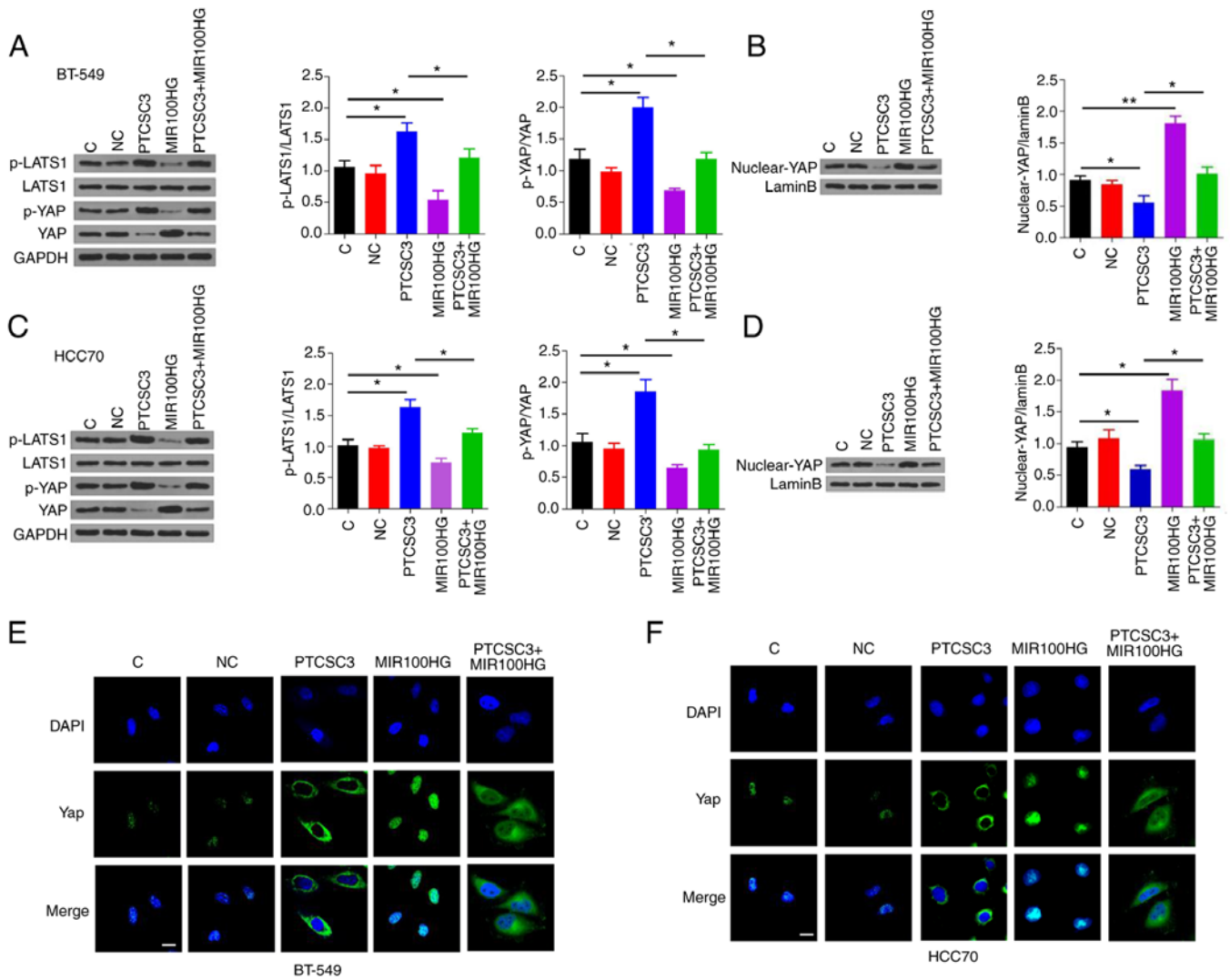


Figure 6. PTSCSC3 suppresses viability and promotes apoptosis of TNBC cell through Hippo signaling pathway. Western blot analysis showed that overexpression of PTSCSC3 led to increased p-YAP/YAP and p-LATS1/LATS1, while overexpression of MIR100HG led to decreased p-YAP/YAP and p-LATS1/LATS1 levels in TNBC (A) BT-549 and (C) HCC70 cells. In addition, rescue experiments showed that overexpression of MIR100HG attenuated the effects of PTSCSC3 overexpression on protein levels. Cell nucleus/cytoplasm fractionation and western blotting analysis were conducted to demonstrate the YAP translocation in (B) BT-549 and (D) HCC70 cells. Immunofluorescence assays showed the localization of YAP in TNBC cells after overexpression with PTSCSC3 or MIR100HG in (E) BT-549 and (F) HCC70 cells. Scale bars, 30 μ m (** P <0.01; * P <0.05). TNBC, triple-negative breast cancer; p-, phosphorylated-; YAP, Yes-associated protein; C, control; NC, negative control.

treatment and prognosis of gastric cancer (29,30), whereas its role in TNBC is unknown. The present study found that lncRNA PTSCSC3 could negatively regulate the expression of MIR100HG and inhibit TNBC cells. Notably, the interaction between MIR100HG and PTSCSC3 was also found in breast cancer cells that are non-triple-negative, indicating that they might also play important roles in other cancer types. However, to date, the functions of MIR100HG and PTSCSC3 in cancer biology have not been fully elucidated and absence of non-cancerous control cells is a limitation in the present study.

It is worth noting that overexpression of MIR100HG only partially rescued the inhibitory effects of PTSCSC3 overexpression on cancer cell viability. Therefore, it is speculated that PTSCSC3 may also interact with other downstream targets to regulate TNBC cell viability. PTSCSC3 inhibits cancer cell migration and invasion in thyroid cancer and glioma (13). However, in the present study PTSCSC3 did not affect the

migration and invasion of TNBC cells. Therefore, PTSCSC3 may have different functions in different types of cancer. In addition, PTSCSC3 inhibited TNBC cell viability and promoted cell apoptosis without affecting cell migration, which can be used to control disease development at early stages. However, the absence of experiments in other tumors is the big limitation of the present study and will be further investigated in other tumors in future studies.

Yes-associated protein (YAP), a downstream regulator of the Hippo pathway, is upregulated in human cancer and is associated with viability, apoptosis, migration, invasion and resistance to chemotherapy drugs in breast cancer (31). It was reported that lncRNA FOXD2-AS1 regulates the tumorigenesis and progression of breast cancer through the S100 calcium binding protein A1/Hippo signaling pathway (32). The present study found that PTSCSC3 regulates TNBC cell viability through the Hippo pathway, which downregulated the phosphorylation level of LATS1 and YAP, and improved the

translocation of YAP. MIR100HG has the opposite effect on PTCSC3 and abolished the effect of PTCSC3. The aforementioned data demonstrated that the Hippo signaling pathway is required for the protective effects of PTCSC3.

In conclusion, PTCSC3 is downregulated in TNBC, and overexpression of PTCSC3 may inhibit TNBC cell viability and promote TNBC cell apoptosis by downregulating MIR100HG. The present study findings might provide a potential target for the prevention and treatment of TNBC.

Acknowledgements

Not applicable.

Funding

No funding was received.

Availability of data and materials

The datasets used and/or analyzed during the current study are available from the corresponding author on reasonable request.

Authors' contributions

GZ and XW conceived and designed the experiments. LG, JZ, RW and XW performed the experiments and analyzed the data. GZ contributed reagents and materials. GZ and XW wrote the manuscript. GZ and XW confirm the authenticity of all the raw data. All authors have read and approved the final manuscript.

Ethics approval and consent to participate

The present study was approved by the Ethics Committee of Changde People's Hospital before the admission of patients. The ethics committee approval number is Changde-20160049. All patients signed the informed consent.

Patient consent for publication

Not applicable.

Competing interests

The authors declare that they have no competing interests.

References

- Djebali S, Davis CA, Merkel A, Dobin A, Lassmann T, Mortazavi A, Tanzer A, Lagarde J, Lin W, Schlesinger F, *et al*: Landscape of transcription in human cells. *Nature* 489: 101-108, 2012.
- Zhao XB and Ren GS: lncRNA Taurine-Upregulated Gene 1 promotes cell proliferation by inhibiting microRNA-9 in MCF-7 cells. *J Breast Cancer* 19: 349-357, 2016.
- Fatica A and Bozzoni I: Long non-coding RNAs: New players in cell differentiation and development. *Nat Rev Genet* 15: 7-21, 2014.
- Engreitz JM, Ollikainen N and Guttman M: Long non-coding RNAs: Spatial amplifiers that control nuclear structure and gene expression. *Nat Rev Mol Cell Biol* 17: 756-770, 2016.
- Gutschner T and Diederichs S: The hallmarks of cancer: A long non-coding RNA point of view. *RNA Biol* 9: 703-719, 2012.
- Spizzo R, Almeida MI, Colombatti A and Calin GA: Long non-coding RNAs and cancer: A new frontier of translational research? *Oncogene* 31: 4577-4587, 2012.
- Peto R, Boreham J, Clarke M, Davies C and Beral V: UK and USA breast cancer deaths down 25% in year 2000 at ages 20-69 years. *Lancet* 355: 1822, 2000.
- Foulkes WD, Smith IE and Reis-Filho JS: Triple-negative breast cancer. *N Engl J Med* 363: 1938-1948, 2010.
- Lin A, Li C, Xing Z, Hu Q, Liang K, Han L, Wang C, Hawke DH, Wang S, Zhang Y, *et al*: The LINK-A lncRNA activates normoxic HIF1 α signaling in triple-negative breast cancer. *Nat Cell Biol* 18: 213-224, 2016.
- Eades G, Wolfson B, Zhang Y, Li Q, Yao Y and Zhou Q: lncRNA-RoR and miR-145 regulate invasion in triple-negative breast cancer via targeting ARF6. *Mol Cancer Res* 13: 330-338, 2015.
- Fan M, Li X, Jiang W, Huang Y, Li J and Wang Z: A long non-coding RNA, PTCSC3, as a tumor suppressor and a target of miRNAs in thyroid cancer cells. *Exp Ther Med* 5: 1143-1146, 2013.
- Wang X, Lu X, Geng Z, Yang G and Shi Y: lncRNA PTCSC3/miR-574-5p governs cell proliferation and migration of papillary thyroid carcinoma via Wnt/ β -catenin signaling. *J Cell Biochem* 118: 4745-4752, 2017.
- Xia S, Ji R and Zhan W: Long noncoding RNA papillary thyroid carcinoma susceptibility candidate 3 (PTCSC3) inhibits proliferation and invasion of glioma cells by suppressing the Wnt/ β -catenin signaling pathway. *BMC Neurol* 17: 30, 2017.
- Wang S, Ke H, Zhang H, Ma Y, Ao L, Zou L, Yang Q, Zhu H, Nie J, Wu C and Jiao B: lncRNA MIR100HG promotes cell proliferation in triple-negative breast cancer through triplex formation with p27 loci. *Cell Death Dis* 9: 805, 2018.
- Xu J, Zhang Y, You Q, Fu H, Zhao X, Lu K, Yan R and Yang D: lncRNA PTCSC3 Alleviates the postoperative distant recurrence of gastric cancer by suppression of lncRNA HOXA11-AS. *Cancer Manag Res* 12: 2623-2629, 2020.
- Livak KJ and Schmittgen TD: Analysis of relative gene expression data using real-time quantitative PCR and the 2^{-Delta}Delta C(T) method. *Methods* 25: 402-408, 2001.
- Fang X, Zhang J, Li C, Liu J, Shi Z and Zhou P: Long non-coding RNA SNHG22 facilitates the malignant phenotypes in triple-negative breast cancer via sponging miR-324-3p and upregulating SUDS3. *Cancer Cell Int* 20: 252, 2020.
- Li Y, Ma HY, Hu XW, Qu YY, Wen X, Zhang Y and Xu QY: lncRNA H19 promotes triple-negative breast cancer cells invasion and metastasis through the p53/TNFAIP8 pathway. *Cancer Cell Int* 20: 200, 2020.
- Luo L, Tang H, Ling L, Li N, Jia X, Zhang Z, Wang X, Shi L, Yin J, Qiu N, *et al*: LINC01638 lncRNA activates MTDH-Twist1 signaling by preventing SPOP-mediated c-Myc degradation in triple-negative breast cancer. *Ocogene* 37: 6166-6179, 2018.
- Chen FY, Zhou ZY, Zhang KJ, Pang J and Wang SM: Long non-coding RNA MIR100HG promotes the migration, invasion and proliferation of triple-negative breast cancer cells by targeting the miR-5590-3p/OTX1 axis. *Cancer Cell Int* 20: 508, 2020.
- Han J, Han B, Wu X, Hao J, Dong X, Shen Q and Pang H: Knockdown of lncRNA H19 restores chemo-sensitivity in paclitaxel-resistant triple-negative breast cancer through triggering apoptosis and regulating Akt signaling pathway. *Toxicol Appl Pharmacol* 359: 55-61, 2018.
- Zuo Y, Li Y, Zhou Z, Ma M and Fu K: Long non-coding RNA MALAT1 promotes proliferation and invasion via targeting miR-129-5p in triple-negative breast cancer. *Biomed Pharmacother* 95: 922-928, 2017.
- Wang N, Hou M, Zhan Y and Sheng X: lncRNA PTCSC3 inhibits triple-negative breast cancer cell proliferation by downregulating lncRNA H19. *J Cell Biochem* 120: 15083-15088, 2019.
- Li P, Ge D, Li P, Hu F, Chu J, Chen X, Song W, Wang A, Tian G and Gu X: CXXC finger protein 4 inhibits the CDK18-ERK1/2 axis to suppress the immune escape of gastric cancer cells with involvement of ELK1/MIR100HG pathway. *J Cell Mol Med* 24: 10151-10165, 2020.
- Huang Y, Zhang C and Zhou Y: lncRNA MIR100HG promotes cancer cell proliferation, migration and invasion in laryngeal squamous cell carcinoma through the downregulation of miR-204-5p. *Onco Targets Ther* 12: 2967-2973, 2019.
- Zhang M, Song Y and Yu L: lncRNA PTCSC3 suppressed cervical carcinoma cell invasion and proliferation via regulating miR-574-5p. *Am J Transl Res* 11: 7186-7194, 2019.

27. Wang XM, Liu Y, Fan YX, Liu Z, Yuan QL, Jia M, Geng ZS, Gu L and Lu XB: lncRNA PTCSC3 affects drug resistance of anaplastic thyroid cancer through STAT3/INO80 pathway. *Cancer Biol Ther* 19: 590-597, 2018.
28. Cai Y, Li Y, Sun B, Wang H, Zhang W, Zhao Y, Zhao H, Zhang J, Xu J and Wang Y: lncRNA PTCSC3 and lncRNA HULC negatively affect each other to regulate cancer cell invasion and migration in gastric cancer. *Cancer Manag Res* 12: 8535-8543, 2020.
29. Hong L, Wang H, Wang J, Wei S, Zhang F, Han J, Liu Y, Ma M, Liu C, Xu Y and Jiang D: lncRNA PTCSC3 inhibits tumor growth and cancer cell stemness in gastric cancer by interacting with lncRNA Linc-pint. *Cancer Manag Res* 11: 10393-10399, 2019.
30. Zhang G, Chi N, Lu Q, Zhu D and Zhuang Y: lncRNA PTCSC3 Is a biomarker for the treatment and prognosis of gastric cancer. *Cancer Biother Radiopharm* 35: 77-81, 2020.
31. Ma J, Fan Z, Tang Q, Xia H, Zhang T and Bi F: Aspirin attenuates YAP and β -catenin expression by promoting β -TrCP to overcome docetaxel and vinorelbine resistance in triple-negative breast cancer. *Cell Death Dis* 11: 530, 2020.
32. Zhang K, Zhang M, Yao Q, Han X, Zhao Y, Zheng L, Li G, Liu Q, Chang Y, Zhang P, *et al*: The hepatocyte-specifically expressed lnc-HSER alleviates hepatic fibrosis by inhibiting hepatocyte apoptosis and epithelial-mesenchymal transition. *Theranostics* 9: 7566-7582, 2019.



Copyright © 2023 Zhang et al. This work is licensed under a Creative Commons Attribution-NonCommercial-NoDerivatives 4.0 International (CC BY-NC-ND 4.0) License.